Novel Hybrid of Clay, Cellulose, and Thermoplastics. I. Preparation and Characterization of Composites of Ethylene–Propylene Copolymer

Annamalai Pratheep Kumar, Raj Pal Singh

Division of Polymer Science and Engineering, National Chemical Laboratory, Pune 411 008, India

Received 23 November 2005; accepted 6 October 2006
DOI 10.1002/app.25659
Published online in Wiley InterScience (www.interscience.wiley.com).

ABSTRACT: The present study is aimed to prepare hybrid materials by incorporating layered silicates and microcrystalline cellulose into thermoplastic polymer. Using ethylene–propylene (EP) copolymer as thermoplastic polymer matrix and maleated EP (MEP) copolymer as compatibilizer, three types of composites were prepared by (i) melt mixing of cellulose with thermoplastics [I], (ii) melt mixing of clay with thermoplastics [II], and (iii) melt mixing of cellulose with the thermoplastic clay nanocomposites [III]. They were characterized by X-ray diffractometry (XRD), differential scanning calorimetry, thermogravimetric analysis, and Fourier transform infrared spectroscopy. Instron was used to measure the mechanical properties. The composites [II] and [III] that contain layered silicates were intercalated nanocomposites as confirmed by XRD and transmission electron microscopy. The improvement in tensile properties was observed in cellulose–fiber-reinforced composites with increasing cellulose content. In nanocomposites [II] and [III], the tensile modulus was improved. The resistance of the cellulose composites [I] for water absorption decreased with increasing content of cellulose fibers. The incorporation of layered silicates reduced the water absorption of cellulose composites. © 2007 Wiley Periodicals, Inc. J Appl Polym Sci 104: 2672–2682, 2007

Key words: cellulose; clay; nanocomposites; mechanical properties; thermal properties; water absorption

INTRODUCTION

There is currently a wide revival of interest in the use of biopolymers for applications in which synthetic polymers have traditionally been the material of choice. Conventional plastics are persistent in the environment and every plastic material disposed improperly is a significant source of environmental pollution, which potentially harms wild life.[1] Bio-based materials have received considerable attention in the past two decades as eco-friendly materials and natural fiber-reinforced composites have been utilized in many applications for last few decades. In natural fibers, cellulose, which is a linear condensation polymer consisting of D-anhydroglucopyranose units linked together by β 1,4-glycoside bond, is major component and other components are lignin, hemicellulose, and water soluble sugars. Conventionally, the composites are made by incorporating natural fibers during processing of the resin in the case of thermoplastics and during polymerization/curing in the case of thermosets. In general, the short fibers (4–10 mm) are utilized as reinforcement to reduce the difficulties during conventional processing conditions and for uniform dispersion throughout the matrix. In recent years, the consumption of these composites has been skyrocketed not only for environmental concerns but also for yielding a unique combination of high performance, great versatility, and processing advantages at favorable cost. They exhibit many advantages including low density, little damage during processing, little requirements on processing equipment, high stiffness, and relatively low price.[2,3] In general, the dramatic improvement by fiber (type) reinforcement is found in dimensional stability.[4–6] The improvement in material properties of the natural fiber-reinforced composites are mostly influenced by the orientation and dispersion of the fiber through out the matrix, individual quality of the fibers, and ultimately the quality of interface.[7] Although fiber reinforcement is much popular due to its abundance, economic viability, easy processability, biodegradability, etc., the incompatibility between the hydrophilic (polar) polysaccharides and hydrophobic (nonpolar) polymer matrix causes the phase separation in these materials. To evade this major problem many efforts have been focused to optimize/influence the quality of the fiber–matrix interface by some physical methods and chemical methods such as change of the surface energy, impregnation, coatings, coupling agents, and graft copolymerization.[8] Among many other

Correspondence to: R. P. Singh (rp.singh@res.in).

Journal of Applied Polymer Science, Vol. 104, 2672–2682 (2007)

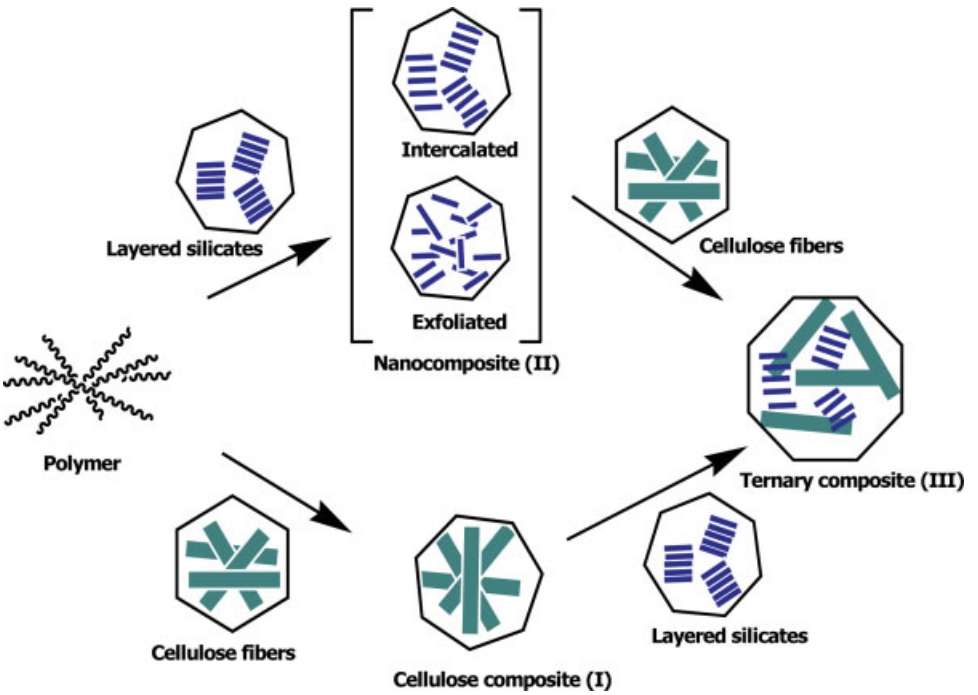

Scheme 1 Schematic representation of the composites prepared. (No scale for size of fillers.) [Color figure can be viewed in the online issue, which is available at www.interscience.wiley.com.]

additives used for this purpose, MAH-PP has been found to be very efficient in improving the filler dispersion and the compatibility in polypropylene–cellulose composites.[7,9,10]

On the other hand, in last few years, reinforcement of nanoscale fillers has been found to improve the physical, thermal, and mechanical properties of the obtained composites with very low amount of loading. The polymer-layered silicate based nanocomposites have received a great deal of interest from researchers from both the scientific and industrial filed. The insertion of polymer chains in the clay platelets that are in the nanometer scale often results in nanocomposites, which exhibit enhanced properties such as improved mechanical properties, heat stability, flame retardency, and gas barrier properties at very low filler content usually less than 5%.[11–14] The improved properties are presumably due to the synergistic effect of the nanoscale structure (high aspect ratio) and the maximized interaction (unique intercalation/exfoliation characteristics) between the filler and polymer molecule. These layered silicates have attracted great attention of researchers because of their low cost, abundance, and high aspect ratio, which give greater possibility of energy transfer from one phase to another.[15] Many attempts are being made to improve the properties of commodity polymers such as polyethylene and polypropylene by nanoclay reinforcement.[16–20] In this system too, the observed problem is incompatibility between polymer (nonpolar) matrix and clay (polar) and thus compatibilization by modifying clay surface, functionalizing polymers, and use of compatibilizers is essentially done.[21]

Considering the dimensional stability from the fiber type reinforcement and the toughness, barrier properties, thermal stability, multidirectional stress transfer (as advantage) from the platelet type reinforcement, in the present work, we have combined both the strategies for reinforcing the synthetic polymers. At the start we used the ethylene–propylene (EP) copolymer. Varying the composition of the monomers in the EP copolymer from soft elastomers to rigid thermoplastics gives a wide range of applications. The EP copolymer and clay nanocomposites were reinforced with cellulose. The preparation of three composites is schematically represented in Scheme 1. Since the compatibilization is essential for this system, the EP copolymer was functionalized as shown in Scheme 2 by maleic anhydride and used as compatibilizer in a constant ratio. The results from Fourier transform infrared spectroscopy (FTIR), X-ray diffractometry (XRD), mechanical property measurements, and thermogravimetric analysis (TGA) of the obtained composites were discussed.

EXPERIMENTAL

Materials

The EP copolymer containing ethylene 15.1% molar content with melt-flow index about 3.5 g/10 min

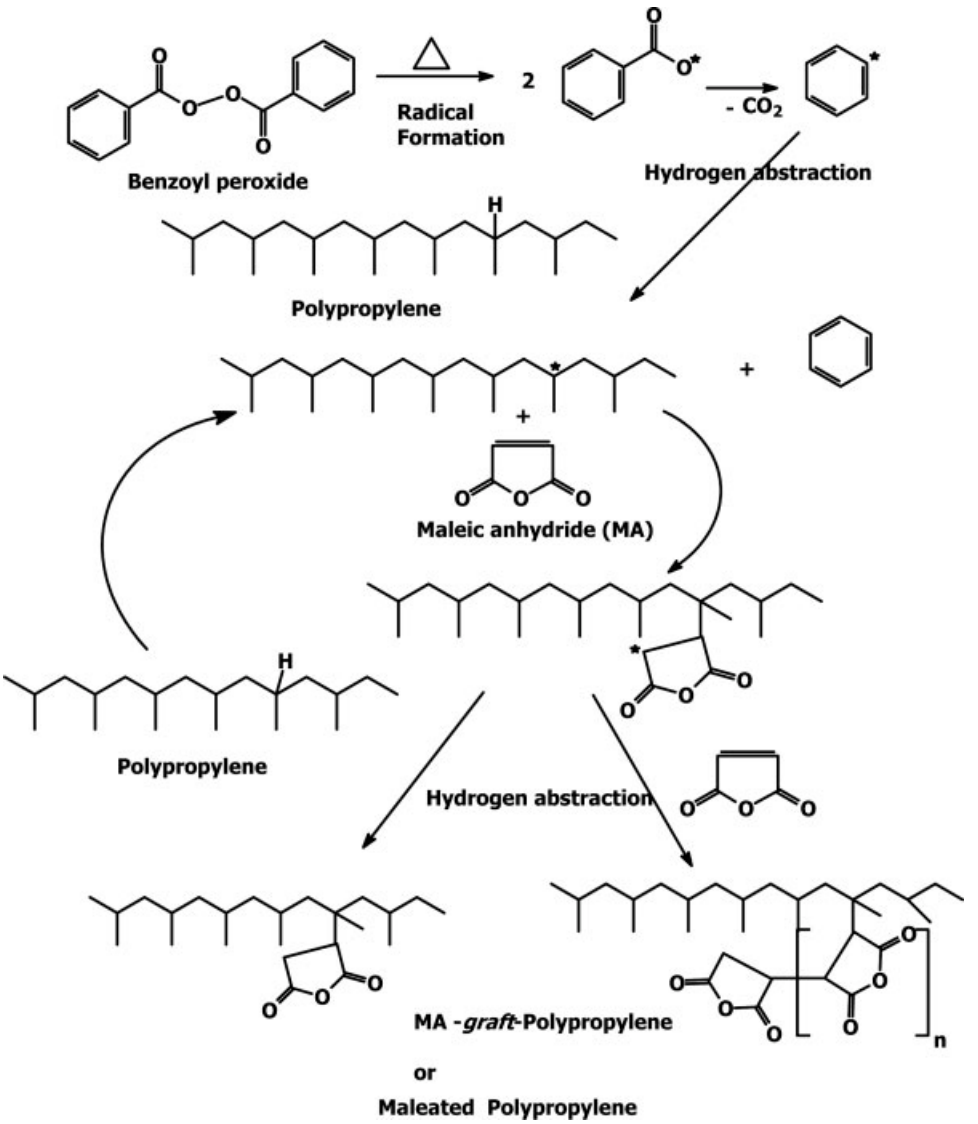

Scheme 2 General reaction mechanism for grafting of maleic anhydride on polyolefins.[22,23]

and density about 0.9 g/cm^3 was obtained from M/s Montell Ferrara, Italia. Maleic anhydride and benzoyl peroxide were obtained from M/s Sd Fine Chemicals, India. Cloisite® 20A that is a natural montmorillonite (designated as MMT20A) modified with dimethyl dehydrogenated tallow quaternary ammonium cation was from M/s Southern Clay Products, USA. The solvents were used as obtained from M/s Sd Fine Chemicals, India. Microcrystalline cellulose was obtained from M/s Loba Chemicals, India.

Preparation

The neat EP copolymer (Neat EP) was functionalized by maleic anhydride grafting or maleation. The vacuum oven dried (at 50°C for 10 h) EP copolymer was melt-mixed in a Brabender (Plasticorder-487106) with presence of benzoyl peroxide (0.15 wt %) and maleic anhydride (5 wt %) at 170°C (65 rpm) for 3 min.

For preparing the first type of composites [I], Neat EP and maleated EP copolymer (MEP) were mixed in the Brabender at 170°C (70 rpm) for 1 min, cellulose (5–15 wt %) was added to this chamber, and the mixing was continued for another 3 min. The composition of Neat EP/MEP was maintained at 60/40 in all type of composites as shown in Table I. The second type of composite [II] was obtained by melt-mixing Neat EP/MEP in the Brabender at 170°C (70 rpm) for 1 min, then 5 wt % of the clay (MMT20A) was added, and the mixing was continued for another 3 min.

The third type of composites was prepared by following the same experimental conditions as used for II. After 2 min of the addition of clay (MMT20A) cellulose fibers (5–15 wt %) were added and allowed to

TABLE I
Composition of Composites Prepared[a]

S. no	Neat EP copolymer (wt %)	Maleated EP copolymer (wt %)	Cellulose (wt %)	Cloisite® 20A (wt %)	Code
1.	100	–	–	–	Neat EP
2.	–	100	–	–	MEP
3.	57	38	5	–	CC05
4.	54	36	10	–	CC10
5.	51	34	15	–	CC15
6.	57	38	–	5	NC05
7.	54	36	5	5	TC05
8.	51	34	10	5	TC10
9.	48	32	15	5	TC15

[a] Where Neat EP/MEP ratio is 60/40. CC, cellulose composite; TC, ternary composite; NC, nanocomposites (i.e. without cellulose).

mix for another 3 min. These composites were sandwiched between two electrically preheated plates covered with aluminum foil in a hydraulic Carver press at 175°C for 2 min keeping the pressure about ~ 15,000 pounds and quench-cooled to room temperature (27°C) for 1 min under pressure. The obtained films were observed to have thickness about 100 ± 10 μm. These films were utilized for further measurements.

Characterization

FTIR spectroscopy

The functional group changes of the samples (as films) were followed using Perkin–Elmer 16 PC FTIR spectrophotometer. The samples were scanned in the range of 4000–400 cm^{-1} at a resolution of 4 cm^{-1}. A total of 10 scans were used for signal averaging.

Mechanical properties measurements

The films were cut according to IS: 2508-1984:A4 for mechanical property investigations. The static tensile behavior of these specimens was investigated at room temperature (27°C ± 2°C) and 65% ± 5% relative humidity using a Universal Testing Machine (Instron model 4204) at crosshead speed at 10 mm/min.

Thermal analysis

The films were cut and used for thermal analysis. The sample weight was about 5 mg. The melting behavior of the samples was analyzed by using Perkin–Elmer DSC-7. The samples were scanned from − 30 to 300°C at the heating rate of 10°C/min and held for 1 min at 300°C and then cooled to 25°C with the same rate.

For measuring the thermal stability, the samples were heated using Perkin–Elmer TGA-7 from 30 to 900°C with a heating rate of 10°C/min under a nitrogen flow rate of 20 mL/min.

X-ray diffraction measurements

The wide-angle X-ray diffraction (WAXD) patterns of the film samples were obtained using a Rigaku Dmax 2500 X-ray diffractometer with Cu-Kα radiation. The system consists of a rotating anode generator with a copper target and a wide-angle powder goniometer having a diffracted beam graphite monochromator. The generator was operated at 40 kV and 150 mA. All the experiments were performed in the reflection mode. The samples were scanned between $2\theta = 2^\circ$–30° at a scan speed of 2°/min. The d spacing was calculated by Bragg's formula where the λ was 0.154 nm.

Microscopic measurements

The dimensions of fibers were determined by using optical microscope (Olympus, Model Bx50 F4, Japan) with 50 × magnification. The diameter of the cellulose fibers was 14.8 ± 0.2 μm and the length was 38.8 ± 0.2 μm. To clarify the nanoscale structure, transmission electron microscopic (TEM) image was obtained by TEM 2000 EX-II instrument (JEOL, Tokyo, Japan) operated at an accelerating voltage of 100 kV to observe the nanoscale morphology. All the ultrathin sections were microtomed using a Super NOVA instrument (M/s Leica, Switzerland) with a diamond knife and then subjected to TEM without staining.

Water absorption

The test specimens were cut according to ASTM D570 (76.2 × 25.4 × 1 mm^3), placed in a vacuum oven at 80°C for 24 h, and then cooled in a dessicator. Immediately after cooling, the specimens were weighed using Prescisa 205 A SCS, Switzerland, with 0.0001 g accuracy and this was considered as the initial weight (W_0). All the specimens were submerged in deionized water for 24 h at 25°C ± 0.2°C.

The specimens were removed after 24 h and immediately wiped with dry clean cotton cloth (to remove water on the surface of the films). Their weights were recorded as final weight (W_1). The water absorption (%) of samples was calculated using the following formula.

$$\left[\frac{\text{Weight of the sample after absorption } (W_1) - \text{Weight of the sample before absorption}(W_0)}{\text{Weight of the sample before absorption}(W_0)}\right] \times 100$$

RESULTS AND DISCUSSION

Characterization of composites

IR spectroscopy

Maleation of polymers is schematically represented in Scheme 2 using polypropylene as an example, which is in higher content in the sample used for this study. The mechanism involves three steps: (i) radical formation from initiator, macromolecular radical formation (by hydrogen abstraction from polymer), (ii) addition of maleic anhydride to yield polymer-chain-substituted succinic anhydride radical which leads to further propagation steps, and (iii) termination via various processes such as radical recombination or disproportionation.[22] During grafting the polyolefins, the product that has been represented in Scheme 2 is the major part.[22,23] Thus, it is essential to analyze the changes at carbonyl group region. Figure 1 shows the FTIR spectra of MEP and cellulose composites. After melt mixing of maleic anhydride with Neat EP, the bands that arise at 1780 and 1853 cm^{-1} for cyclic anhydride and the band at 1713 cm^{-1} for carboxylic acid dimer indicate the maleation of EP copolymer [Fig. 1(a)]. It was further confirmed by the decrease in the absorbance of the bands at 1363 and 1580 cm^{-1}, which is attributed to the absence of the anionic form of carboxylic acid dimer in MEP. In type [I] composites the decrease in the absorbance of the 1780 cm^{-1} band (cyclic anhydride) and the appearance of bands at 1740–1720 cm^{-1} (stretching of ester C=O) are attributed to the ester formation [Fig. 1(b)]. This absorption was found to increase with increasing content of cellulose fibers. The ester formation that is one of the supporting evidences for compatibility[7] depends on the availability of hydroxyl groups on the surface of the fibers. The higher absorbance at hydroxyl region (3300–3475 cm^{-1}) was observed with increasing content of cellulose, which is attributed to the hydrogen bonded hydroxyl groups of cellulose.

Figure 2 shows the IR spectra of type [II] (clay reinforced) and [III] (ternary) composites and they are compared with IR spectrum of CC05. The bands at 670 cm^{-1} and 1230–1250 cm^{-1} regions are assigned for the deformation and stretching of the Si—O bond. The absorbance for bending vibrations of the Si—O bond of smectite clays can be observed in the 522–466 cm^{-1} region. In addition, the free hydroxyl group

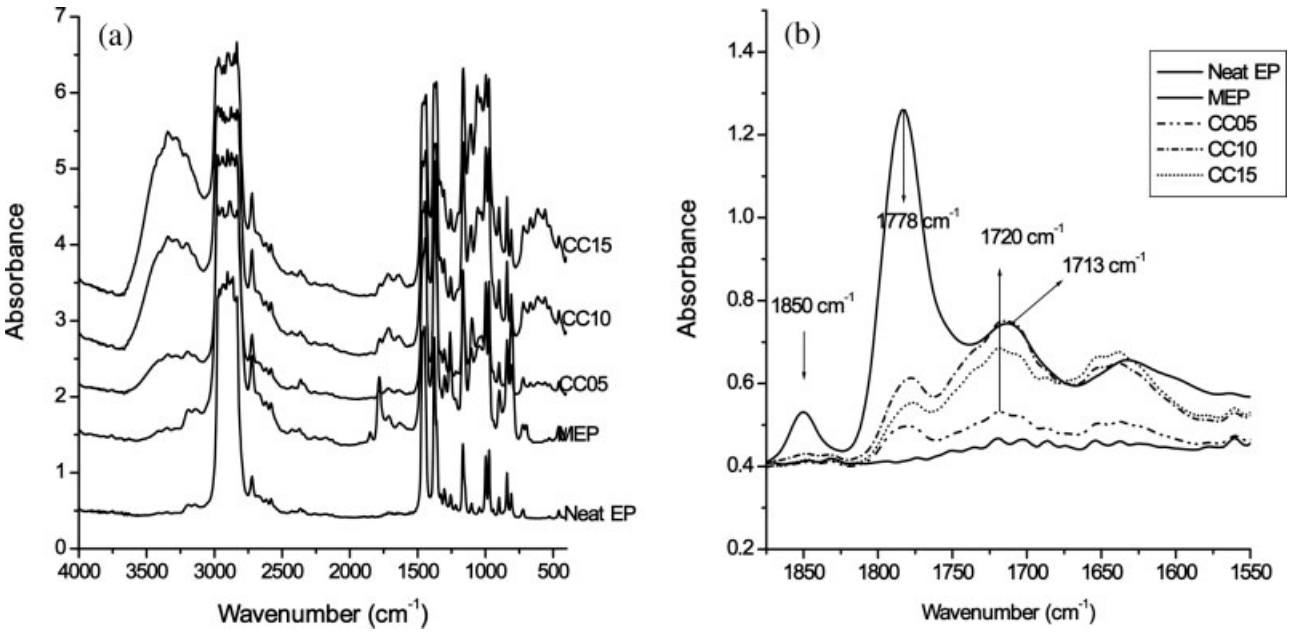

Figure 1 FTIR spectra of cellulose composites: (a) full (4000–400 cm^{-1}) and (b) expanded carbonyl region.

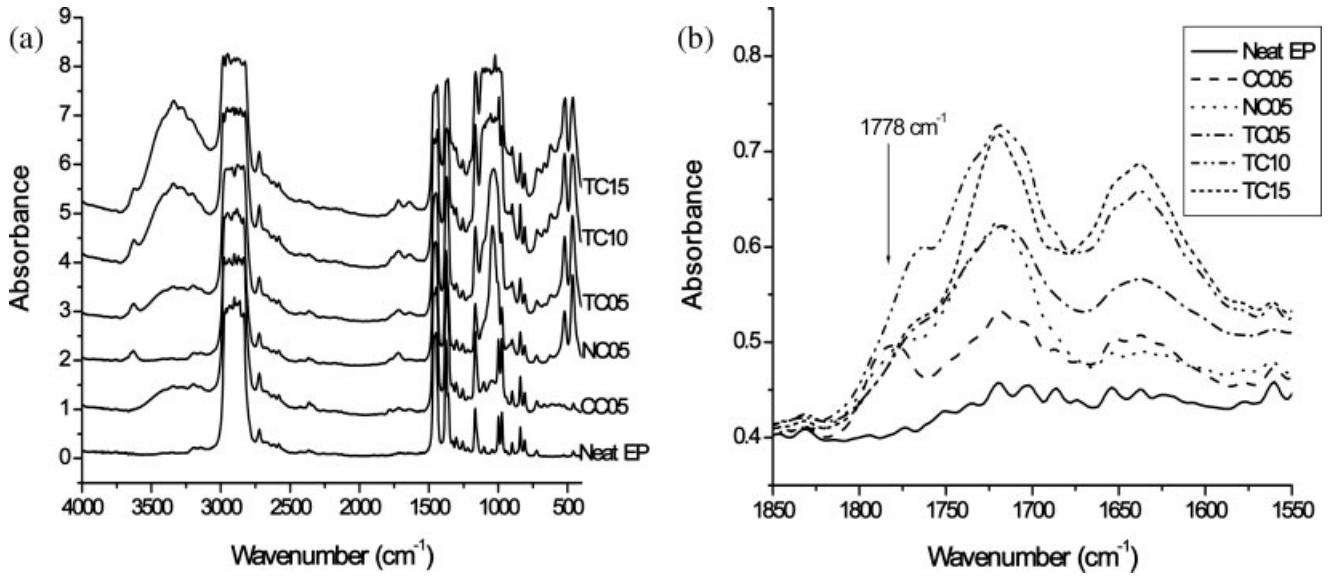

Figure 2 FTIR spectra of clay containing (type [II] and [III]) composites: (a) full and (b) expanded carbonyl region.

band of the inorganic layered silicate was seen at 3600 cm^{-1}. Figure 2(b) shows the absorbance peaks of the ester region for the clay containing composites.

Morphology and structure by XRD and TEM

The characteristics of interaction (i.e., intercalation, exfoliation, flocculation, or microcomposites) between polymer chains and layered silicates could be analyzed by XRD and TEM tools. The shift in peaks of 001 basal plane from higher angle ($2\theta = 4^\circ$–6°) to lower angle ($2\theta = 1.5^\circ$–3°) typically represents the *d* spacing between the silicate layers. The increase in the *d*-spacing indicates the crawling of macromolecular chains into the gallery of layered silicates that is generally called as ''intercalation,'' while delamination of these silicate layers from the gallery order can be called as ''exfoliation'' for which no peaks at lower angles will be observed.

The WAXD patterns of the samples can be seen in Figure 3. The peaks at about 2θ 16° and 23° are observed for neat cellulose crystalline fibers. These peaks in other samples were hardly detectable, which may be due to the destruction of crystalline region of cellulose during processing or by reaction with the compatibilizer used. The interlayer *d*-spacing in the clay (MMT20A) was observed at about 23.23 Å($2\theta = 3.8^\circ$). In NC05, basal-spacing of the 001 plane was found to be 28.48 Å($2\theta = 3.1^\circ$), which indicates that the melt-mixing of Neat EP and MEP with MMT20A resulted in the ''intercalation'' of the polymer chains into the galleries. This increase was also noted in

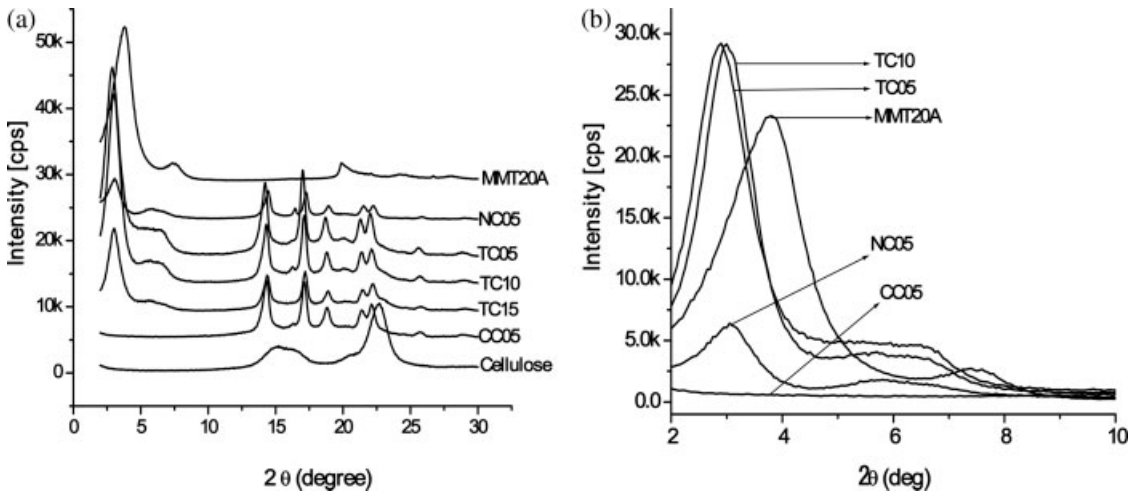

Figure 3 X-ray diffraction patterns of composites from the range of (a) 2°–30° and (b) 2°–10°.

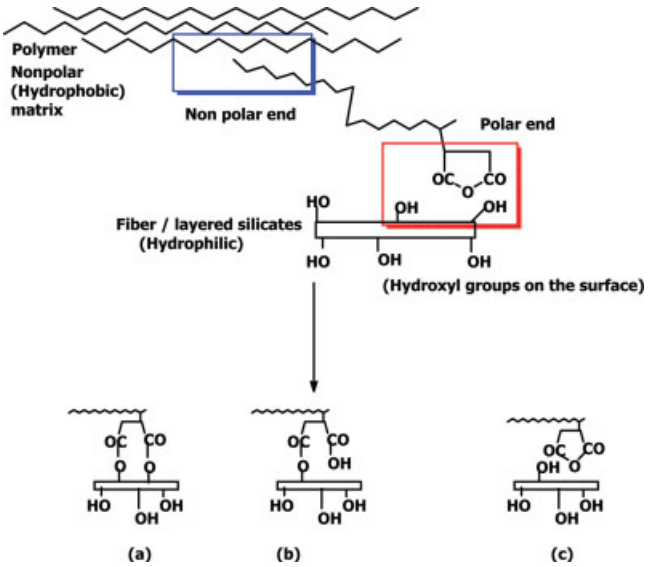

Scheme 3 Possible interactions of compatibilizer with polymer matrix and fillers.[7,24] [Color figure can be viewed in the online issue, which is available at www.interscience.wiley.com.]

TC05 where the *d*-spacing was about 30.44 Å($2\theta = 2.1^\circ$). This can be attributed to the increased melt-mixing time (5 min), as the time of dispersion in melt-stage facilitates the crawling of polymer chains in between the silicate layers. Further increase in *d*-spacing was not observed in the case of TC10 and TC15 and they show the same value of *d*-spacing of about 29.42 Åat $2\theta = 3.0^\circ$, which is lesser than that of TC05. This can be correlated to the availability of succinic anhydride groups of MEP, which are reactive and interact with both cellulose fiber and clay. According to Hasegawa et.al.[16,17] on using the maleated polyolefins as compatibilizer for the polyolefin–clay nanocomposites, the acid anhydride content, molecular weight of compatibilizer, and composition used in preparation are the factors strongly influencing the formation of nanocomposites. The possible interactions of fillers, compatibilizer, and polymer are schematically represented in Scheme 3. The interactions (a) and (b) result in the formation of covalent bond between the compatibilizer and fibers. The complete ester formation could be predominantly favored by solution-impregnation method, while by melt-mixing method, the esterification reaction could occur in lesser extent. Thus, in the prepared composites, just the polar–polar interactions (c) may also possibly be present.[7,24] However, the increase in the cellulose content makes available the organic hydroxyl groups for the reaction with acid anhydride groups of MEP. The reaction of these acid anhydride groups with cellulose leads to increase in mass value, which may ultimately result in the decrease in the transformation. In other words, mobility of the macromolecular chains may be reduced, thus reducing the confinement of the polymer chains into the silicate galleries. Thus, it is assumed that in composites with constant ratio of polymer and compatibilizer, the increasing cellulose content may not favor the confinement of polymer chains into silicate galleries.

The bright field TEM image of the type [III] composite TC05 is represented in Figure 4. It shows the characteristic platelets of the montmorillonite (MMT) tactoids, in which the dark entities are the cross section of intercalated MMT layers and bright areas represent the polymer matrix.

Mechanical properties

Table II and Figure 5 depict the variations in the mechanical properties of the composites with different fillers. The modulus that expresses the stiffness of a material was observed to be linear with the concentration of cellulose fibers. In Figure 5(a), with the same amount of loading of fillers (5 wt %), NC05 has shown higher modulus value than CC05, indicating that the clay is a better reinforcer than microcrystalline cellulose due to higher aspect ratio of nanosized platelets. It has been well[25,26] explained that the higher surface area [$\sim$ 760 m^2/g] of layered silicates allows more polymer–filler interactions, which facilitate the stress transfer to the fillers than in the case of cellulose microcrystals. The yield stress, indicating the hardness of the material, has been found to improve, when the cellulose fibers were reinforced in comparison of the neat polymer matrix. Figure 3(b) shows the linear increase in the yield stress with the incorporation of cellulose fibers (CC05–CC15), indicating that the cellulose fibers improve the stress resistance of the samples. Then, NC05 in which MMT20A is incorporated (5 wt %) shows the increase in yield stress, but the value was not higher than that of cellulose composite CC05.

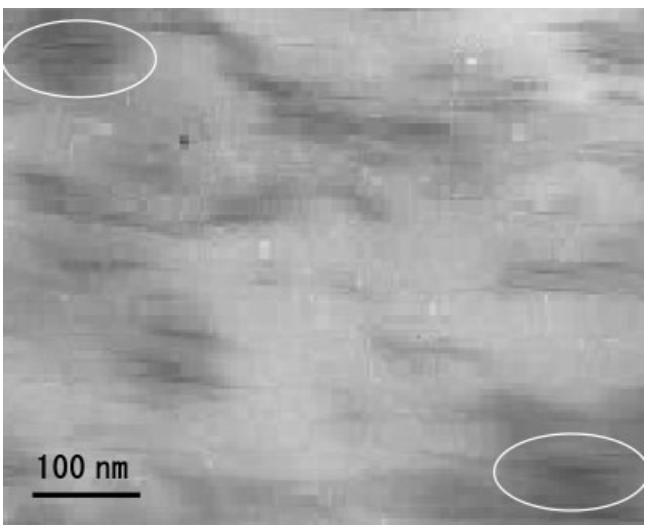

Figure 4 Bright field TEM image of TC05 composite.

TABLE II
Effect of Reinforcement on the Mechanical Properties

	Modulus		Stress at yield		Stress at break	
Sample	MPa	Improvement (%)	MPa	Improvement (%)	MPa	Improvement (%)
Neat EP	773	–	15.9	–	14.8	–
MEP	816	5.5	17.8	12.3	16.7	12.6
CC05	1040	34.5	24.5	54.1	22.9	54.5
CC10	1260	65.5	25.7	61.9	23.6	59.0
CC15	1515	95.9	29.0	82.2	27.3	84.2
NC05	1202	55.5	19.7	24.2	14.4	−2.8
TC05	1240	60.4	17.8	12.3	17.3	16.7
TC10	1397	80.7	18.3	15.4	18.0	21.6
TC15	1622	109.8	19.3	21.8	18.6	25.2

Type [III] composites also show the lower values of yield stress than their counterparts of cellulose composites (Type [I]). In other words, the incorporation of clay with cellulose composites decreases the yield stress of the samples, indicating that the applied stress is not efficiently transferred in ternary composites. Obviously, it is contrary to our expectation. This peculiar behavior may be attributable to increasing content of various fillers (phases). With the constant ratio of polymer matrix and compatibilizer, increasing content of the cellulose fibers, in ternary composites, acid anhydride groups of compatibilizer may mostly interact with organic hydroxyl groups from the cellulose fibers. This may reduce the interaction (i.e., compatibilization) with inorganic silicate layers. This may also be the reason for

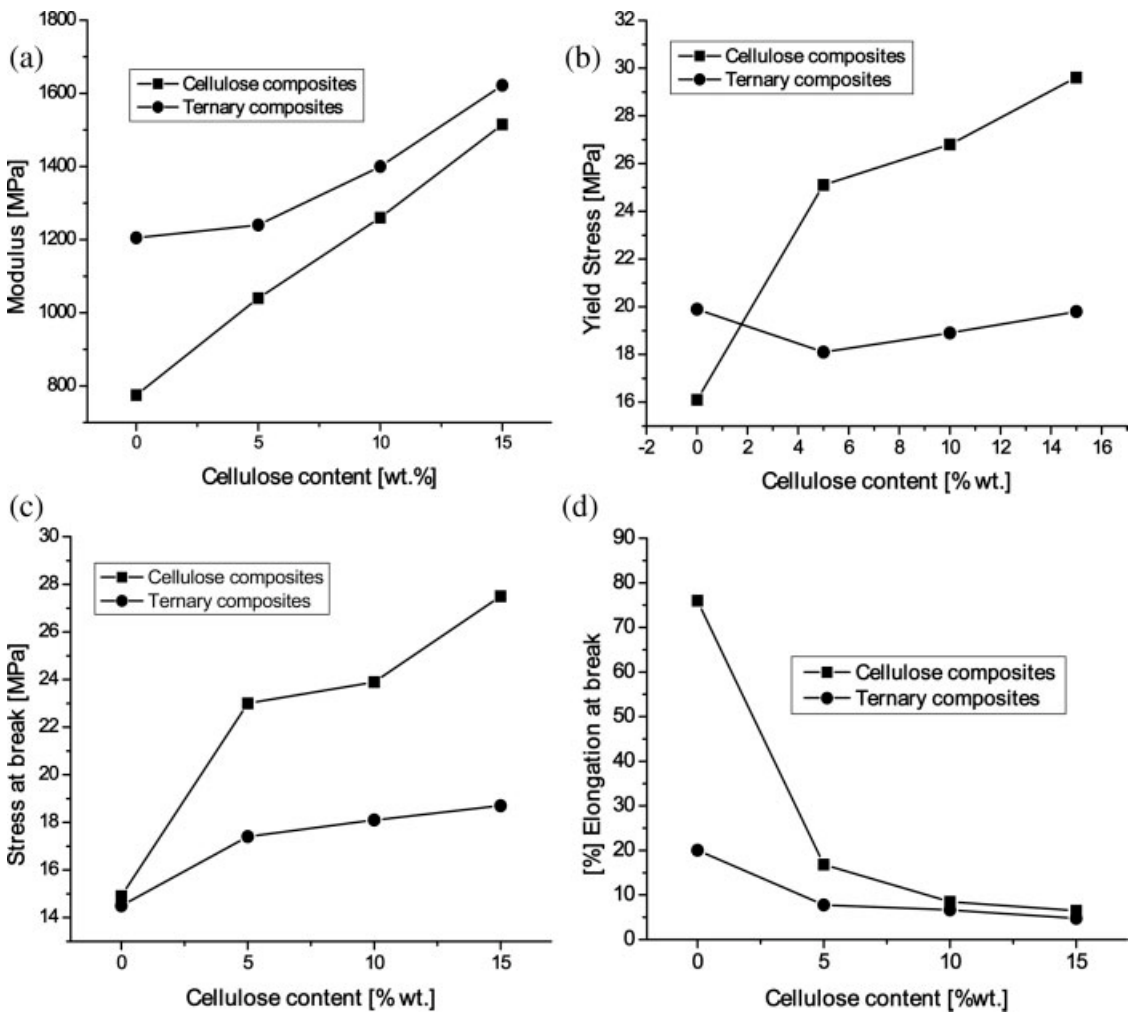

Figure 5 Influence of layered silicates on mechanical properties: (a) tensile modulus, (b) yield stress, (c) stress at break, and (d) elongation at break.

TABLE III
Melting and Decomposition Temperatures

Sample	T_m (°C)	T_d (°C) EP
Neat EP	165.8	453.3
MEP	166.5	443.2
CC05	166.7	458.1
CC10	168.2	461.1
CC15	168.7	463.1
NC05	165.7	458.9
TC05	167.6	466.4
TC10	169.3	483.3
TC15	170.0	482.1

nonexpanding behavior of silicate layers as it was observed in WAXD patterns of TC10 and TC15. Thus, the reduced interaction between clay and macromolecular chains may result in agglomeration of layered silicates. Even for TC05 (5 wt % cellulose), as it can be seen in TEM image, some part of the silicate layers (dark entities) seem to be continuous indicating the agglomeration of silicate layers. This agglomeration is believed to cause the phase separation and ultimately decrease in yield stress.

Kazayawoko et al.[27] demonstrated that only the chemical compatibility such as ester bond formation between hydroxyl group of fibers and anhydride group of compatibilizer is not the key determining factor for enhancing the mechanical properties. The other factors, which improve the mechanical properties, may be reduction in surface energy, polarity, and mechanical interlocking of compatibilizer and filler.[27,28] The detrimental effect of incompatibility can be found in decrease in stress at break that is the ultimate strength of the material [Fig. 5(c)]. With increasing cellulose content (CC05–CC15) the ultimate strength values increased linearly in the cellulose composites. The lower stress at break was found for polymer–clay nanocomposite (NC05) than cellulose composite (CC05). It is reflecting the results of Hasegawa and coworkers.[16,17] Ternary composites (TC05–TC15) exhibited lower ultimate strength values than their counter parts of cellulose composites. Figure 5(d) shows that the elongation (%) at break decreased in both cellulose composites and clay containing composites. The elongation (%) at break, which denotes the ductility of samples, decreases about 76%, when the cellulose is reinforced (CC05). Further reinforcement of clay decreases the elongation values adversely. The decrease in elongation was due to the restriction in momental velocity of polymer chains, as the chains were in sandwiched form in the silicate galleries. It appears that during the tensile test under applied stress the macromolecular chains may undergo three steps that are uncoiling, stretching, and slippage. These are restricted in nanocomposites due to the stretching and confinement of polymer chains in the silicate galleries. Under applied stress, the ''incompatible centers,'' created due to incorporation of different fillers, initiate failure by causing the local stress in their vicinity to exceed the strength of the material at early stages of the tensile tests. Predominantly, the mechanical properties (other than elongation (%)) of the cellulose composites were found to be higher than neat EP copolymer matrix. the mechanical properties of natural fiber-reinforced composites except tensile modulus decreased with the incorporation of clay. However, the usefulness of the polymeric material in many applications is largely determined by its predominant failure mechanism under the conditions of applications. In the tensile test, the neat polymer films were believed to follow the craze failure mechanism that require the mobility of molecular chains to absorb more energy, while the reinforced composites could be considered to follow the crack mechanism.[29,30] This crack mechanism can be expected to indicate the brittle nature of samples.[31] The optimization of interface quality for better mechanical properties is under progress by using different composition of fillers and compatibilizer.

Thermal analysis

The thermal behavior of these composites, which were analyzed by differential scanning calorimetry (DSC) and TGA, can be seen in Table III and Figures 6 and 7. Figure 6 shows the DSC thermograms of the samples and melting point for the neat EP copolymer was observed at ~165°C. In the composites, no significant change in melting point was observed with increasing amount of fillers. The marginal increase in melting point of clay containing composites (TC05–TC15) may be attributed to the heat deflection property of layered silicates and restriction of thermal

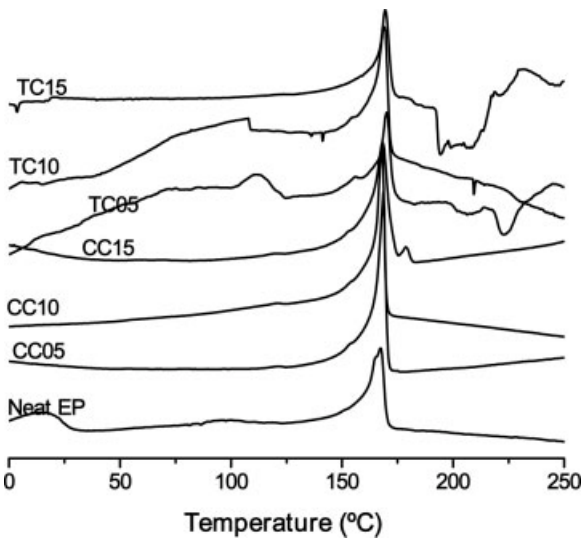

Figure 6 DSC thermograms of the samples.

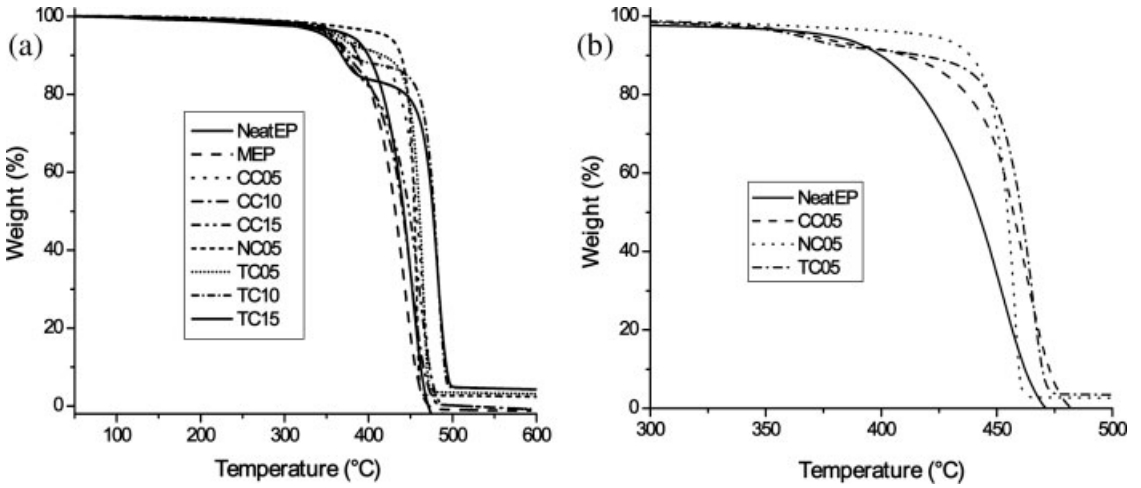

Figure 7 TGA thermograms of the composites under nitrogen: (a) all samples (50°C–600°C) and (b) expanded at 300°C–500°C region.

motion of the macromolecular chain in the silicate layers.[32,33] According to Tyan et al.[34] upon melting, thermal expansion in nanocomposites is reduced because the macromolecular chains that are sandwiched in between silicate layers and plane (platelet)-oriented tend to relax in a direction normal to its original direction. This may be because the silicate layers are much more rigid in nature than polymer molecules and they do not deform and it becomes difficult for polymer molecules to relax. In ternary composites, transitions above the melting point of the matrix may be explained by the assumption that the layered silicates and increasing concentration of cellulose fibers increase the phase separation and apparently accelerate the heterogeneous nucleation to crystallize at higher temperatures by acting as nucleation centers.[35]

Table III shows the maximum decomposition of (host) matrix T_d (°C) for all the samples. It can be observed that the decomposition temperature of MEP is lower than Neat EP and this can be attributed to the functional moieties such as acid anhydride that can facilitate the degradation. In cellulose containing composites, although the initial decomposition starts about 350°C, the maximum decomposition of the host matrix takes place at a higher temperature than the neat polymer. In cellulose composite (CC05) as well as in the nanocomposites NC05, T_d was observed to be about 5°C more than the neat polymer matrix. The same effect could be found in the case of ternary composite (TC05) where the increase was found to be about 13°C in comparison to the polymer matrix. The increase in T_d for clay containing composites was due to well explained by several authors.[34,36,37] They have shown that the diffusion of degraded products might be slowed down/restricted in between the silicate galleries. The reduction of thermal mobility of molecules by silicate layers depends on the orientation of polymer molecules, the rigid nature of the silicate layers, and their integrity. However, the observed increase in decomposition temperature may not be significant for improving the thermal stability of natural fiber-reinforced composites.

Water absorption behavior

The water absorption behavior is an important parameter to be examined, when we deal with hydrophilic cellulose fiber-reinforced thermoplastic composites. Higher water uptake of the composite worsens the mechanical properties and changes the dimensional stability of articles by swelling.[38] Figure 8 shows the percentage water absorption for all the systems, where it can be seen that water was found to be absorbed more in the case of composites than the neat polymer. It is observed that with constant ratio of polymer and compatibilizer, the increasing

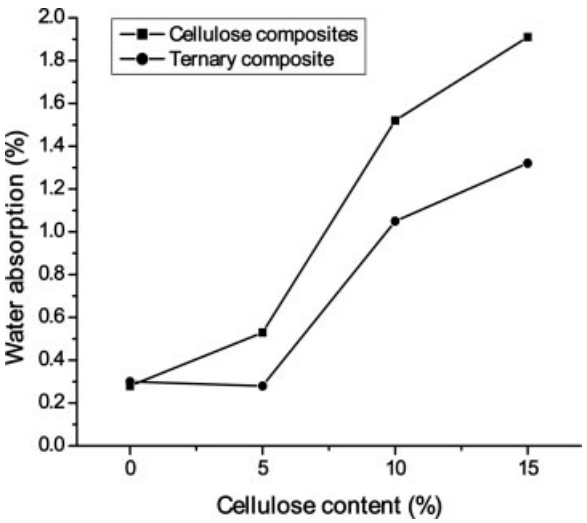

Figure 8 Water absorption behavior of all samples (24 h immersion).

cellulose content increases the water absorption. This may be due to the hydrophilic nature of cellulose. The incorporation of layered silicates decreases the water uptake into the composites. Generally, the layered silicates are rich in water content. The clay used in this work was hydrophobically modified. The reduction in absorption may be due to the presence of completely immobilized clay and partially immobilized polymer chains on the amorphous region. Tsagaroulos and Eisenberg[39] have well explained the concept of these kind of phases in favor of reduction of water absorption. Thus, it is assumed that the presence of layered silicates may reduce the water absorption of cellulose composites.

CONCLUSIONS

In the present study, we have tried to find possibilities of reinforcing thermoplastic polymer matrix with both cellulose fibers and layered silicates. The nanoclay reinforcement is well known for its higher performance in polymeric materials. The improvement in material properties such as mechanical, thermal, and water absorption properties was observed in cellulose-reinforced composites (Type [I]) as well as layered silicates-reinforced composite (Type [II]). The incorporation of layered silicates and cellulose fibers into EP copolymer matrix has increased the thermal stability significantly and melting temperature marginally. This increase is observed particularly when the polymer molecules were intercalated into the silicate layers. Tensile modulus of the ternary composites was improved markedly as compared to the neat polymer matrix and the cellulose composites. But, the other mechanical properties such as ultimate strength and elongation (%) were drastically decreased. Because of the hydrophilic nature of the cellulose fibers, the water absorption of cellulose-reinforced composites (Type I) was increased with increasing content of cellulose. The slight reduction in water absorption was observed after incorporating the layered silicates into cellulose-reinforced composites. However, the improvement in the thermal and mechanical properties observed in the present study may not contribute significantly to the structural applications. The optimization of conditions for better material properties and the evaluation of their durability under different environmental conditions are under investigation.

The authors are grateful to Dr. S. Sivaram, Director, National Chemical Laboratory, Pune, India, for his fruitful discussions and encouragement and to Dr. C. Ramesh for XRD facility and his valuable suggestions. A.P. Kumar is thankful to Council of Scientific and Industrial Research (CSIR), New Delhi, India, for granting him Senior Research Fellowship (SRF) during this study.

References

1. Scott, G. In Degradable Polymers Principles and Applications; Scott, G.; Gillead, D., Eds.; Chapman Hall: New York, 1995; Chapter 13.
2. Joyly, C.; Kofman, M.; Gauthier, R. J Macromol Sci A 1996, 33, 1981.
3. Zadorecki, P.; Michell, A. J. Polym Compos 1989, 10, 69.
4. Elvy, S. B.; Dennis, G. R.; Ng, L. T. J Mater Process Technol 1995, 48, 365.
5. Gauthier, R.; Joly, C.; Coupas, A. C.; Gauthier, H.; Escoubes, M. Polym Compos 1998, 19, 287.
6. Maldas, D.; Kokta, B. V. J Appl Polym Sci 1991, 42, 1443.
7. Felix, J. M.; Gatenhom, P. J Appl Polym Sci 1991, 42, 609.
8. Bledzki, A. K.; Gassan, J. Prog Polym Sci 1999, 24, 221.
9. Joyly, C.; Kofman, M.; Gauthier, R. Comp Sci Technol 1996, 56, 76.
10. Amash, A.; Zugenmaier, P. Polym Bull 1998, 40, 25.
11. Okada, A.; Fukushima, Y.; Kawasumi, M.; Inagaki, S.; Usuki, A.; Sugiyama, S.; Kurauch, T.; Kamigaito, O. U.S. Pat. 4,739,007 (1998).
12. Kojima, Y.; Usuki, A.; Kawasumi, M.; Okada, A.; Fukushima, Y.; Kurauchi, T.; Kamigaito, O. J Mater Res 1993, 8, 1185.
13. LeBaron, P. C.; Wang, Z.; Pinnavaia, T. J. Appl Clay Sci 1999, 15, 11.
14. Alexandre, M.; Dubois, P. Mater Sci Eng R: Rep 2000, 28, 1.
15. Ray, S. S.; Okamoto, M. Prog Polym Sci 2003, 28, 1539.
16. Hasegawa, N.; Kawasumi, M.; Kato, M.; Usuki, A.; Okada, A. J Appl Polym Sci 1998, 67, 87.
17. Kawasumi, M.; Hasegawa, N.; Kato, M.; Usuki, A.; Okada, A. Macromolecules 1997, 30, 6333.
18. Manias, E.; Touny, A.; Wu, L.; Strawhecker, K.; Lu, B.; Chung, T. C. Chem Mater 2001, 13, 3516.
19. Wang, K. H.; Choi, M. H.; Koo, C. M.; Choi, Y. S.; Chung, I. J. Polymer 2001, 42, 9819.
20. Liu, X.; Wu, Q. Polymer 2001, 42, 10013.
21. Mishra, J. K.; Hwang, K. J.; Ha, C. S. Polymer 2005, 46, 1995.
22. Moad, G. Prog Polym Sci 1999, 24, 81.
23. Roover, B. D.; Sclavons, M.; Carlier, V.; Devaux, J.; Legras, R.; Momtaz, A. J Polym Sci Part A: Polym Chem 1995, 33, 829.
24. Kumar, A. P.; Depan, D.; Singh, R. P. J Thermoplast Compos Mater 2005, 18, 489.
25. Messersmith, P. B.; Giannelis, E. P. Chem Mater 1994, 6, 1719.
26. Messersmith, P. B.; Giannelis, E. P. J Polym Sci Part A: Polym Chem 1995, 33, 1047.
27. Kazayawoko, M.; Balatinecz, J. J.; Matuana, L. M. J Mater Sci 1999, 34, 6189.
28. Keener, T. J.; Stuart, R. K.; Brown, T. K. Compos Part A: Appl Sci Manuf 2004, 35, 357.
29. Kramer, E. J. Adv Polym Sci 1983, 52/53, 1.
30. Kumar, A. P.; Singh, R. P.; Sarwade, B. D. Mater Chem Phys 2005, 92, 458.
31. Bicerano, J. Prediction of Polymer Properties, 3rd ed.; Marcel Dekker: New York, 2002.
32. Blumstein, A. J Polym Sci Part A: Gen Pap 1965, 3, 2665.
33. Burnside, S. D.; Giannelis, E. P. Chem Mater 1995, 7, 1597.
34. Tyan, H.-L.; Liu, Y.-C.; Wei, K.-H. Chem Mater 1999, 11, 1942.
35. Amash, A.; Zugenmaier, P. Polymer 2000, 41, 1589.
36. Bharadwaj, R. K.; Mehrabi, A. R.; Hamilton, C.; Trujillo, C.; Murga, M.; Fan, R.; Chavira, A.; Thompson, A. K. Polymer 2002, 43, 3699.
37. Tidjani, A.; Wald, O.; Pohl, M. M.; Hentschel, M.P.; Schartel, B. Polym Degrad Stab 2003, 82, 133.
38. Qiu, W.; Zhang, F.; Endo, T.; Hirotsu, T. J Appl Polym Sci 2003, 87, 337.
39. Tsagaroulos, G.; Eisenberg, A. Macromolecules 1995, 28, 6067.